JOURNAL OF MATERALS SCIENCE 33 (1998) 3919–3925

Measurement of the activation enthalpies of ionic conduction in apples

F. X. HART, V. SCHMIDT
The Department of Physics, The University of the South, Sewanee, TN 37383, USA
E-mail: fhart@sewanee.edu

L. RAY, E. SHRUM
Science Department, Grundy County High School, Tracy City, TN 37387, USA

Impedance spectra in the range from 10 Hz to 1 MHz were obtained for apples for temperatures between 4 and 40 °C. At each temperature the measured spectrum was fitted to a theoretical model in which the bulk properties of the apple were represented as the parallel combination of a constant phase element and a resistance. The results were used to determine the activation enthalpies of apples for ionic migration, H_m, and for dissociation of an ion from its binding site, H_f. H_m was found to be of the order of 0.15 eV whereas H_f was of the order of 0.03 eV. Changes in the slope of the activation curves indicated that a structural change occurred in the cell wall within the temperature range between 35 °C and 40 °C.

1. Introduction

Impedance spectroscopy and dielectric spectroscopy are two widely used, closely related, experimental techniques for measuring the variation of the electrical properties of a material with frequency. These methods are well-suited for monitoring the internal changes in the physical properties of a system caused by the variation of independent parameters, such as temperature or time. These techniques have been applied to a wide variety of physiological processes in biological materials, ranging from impedance changes in canine kidney cells upon removal of calcium ions [1], to changes in palmar skin phase angle after exercise [2], to the measurement of whole-body fluid volumes [3]. Variations in the passive electrical properties of living biomaterials can be correlated with changes in physiological processes at the cellular level and can thus provide information regarding the mechanisms of these processes. In this manner, changes at the cellular level may be studied in intact, living tissue rather than in an artificial environment in cell culture dishes.

In biological materials, the fundamental electrical properties, conduction and polarization, are determined by the "detrapping" and subsequent "hopping" of ions. The correlation of cellular changes with electrical properties then requires that a relationship be determined between ion detrapping and hopping and the physiological state of the system. Measurement of the electrical properties as a function of temperature provides a means for separating the contributions of detrapping and hopping, as well as a method for identifying the existence of changes in the structural state of the membrane, along which the charge transport takes place.

The purpose of this paper is to describe the measurement of the enthalpies for ionic conduction in apples. In particular, it compares the relative importance of the energy needed to generate additional free charge carriers (detrapping) and the energy needed to maintain transport (hopping) of the mobile ions. Furthermore, the variation in the electrical parameters is examined to determine whether there is evidence for the presence of a phase change in the cell wall between 34 and 42 °C.

Sharp changes in the electrical properties of biological systems over a narrow temperature range have been reported recently. McRae and Esrick [4] have shown that the low-frequency electrical impedance of rat skeletal muscle decreased abruptly after hyperthermia. A rapid, initial decrease was attributed to the shrinking of cells with a corresponding increase in extracellular space and to the leaking of intracellular fluid through the membrane. A subsequent, slower decrease was attributed to histolysis. An Arrhenius analysis identified two activation energies: 36.1 kcal mol^{-1} (1.57 eV) above 43 °C and 58.3 kcal mol^{-1} (2.54 eV) below 43 °C.

Bao *et al.* [5] measured the electrical parameters of human erythrocytes between 4 and 40 °C. They observed a marked change in membrane capacitance at 37 °C, which they attributed to a possible phase transition.

2. Experimental procedure

The basic measuring system is an enhancement of the system described in earlier papers for the measurement of the electrical properties of plant and animal

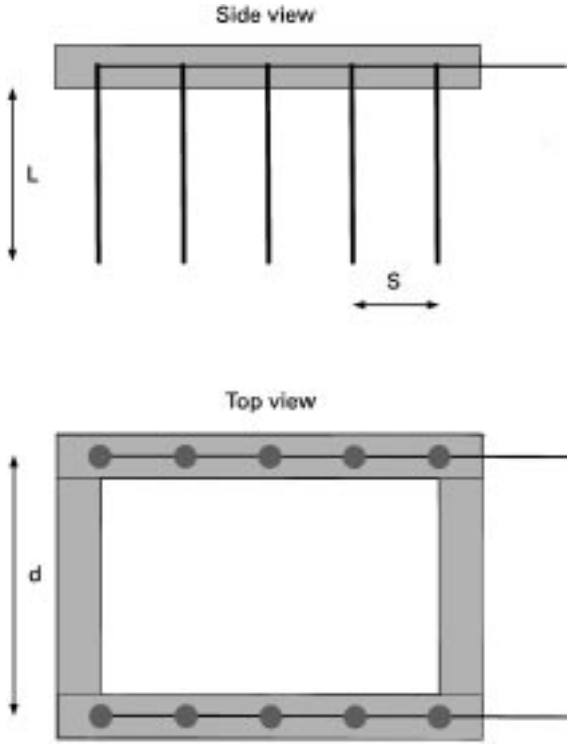

Figure 1 Schematic diagram of the electrodes. The shaded regions represent plastic blocks which provide mechanical rigidity. *L*, *s*, and *d* represent, respectively, the length and spacing of the needles and the separation of the electrodes.

tissues [6–10]. Fig. 1 is a schematic diagram of the electrodes used in the study. Two electrodes are inserted into a material. Each electrode is a co-planar set of five nickel-plated steel sewing needles ($L = 2.0$ cm long, 0.73 mm diameter, and spaced $s = 1.0$ cm apart). The separation of the electrodes, d, is 3.0 cm. The rectangular area defined by each electrode, S, is 8.0 cm^2. The blunt ends of the needles of each electrode are connected by thin wires and embedded in a plastic block. The two blocks, in turn, are connected at the ends by plastic pieces. In this manner mechanical rigidity of the electrode system is achieved. The electrodes cannot be regarded simply as a pair of parallel plates of separation d and area S. The geometrical factor that must be included in order to account for the actual current paths between the needles will be noted later.

The electrodes are connected to a Hewlett Packard 4192A low-frequency impedance analyser. Capacitance, $C(f)$, and conductance, $G(f)$, spectra are measured at 100 frequencies, f, between 10 Hz and 1 MHz. The process is controlled by a Hewlett Packard Model 310 personal computer. The data are transferred to another computer for more detailed analysis with the spreadsheet program Excel.

The apples used in this study were the Red Delicious variety and were purchased at a grocery store. Two apples were removed from a refrigerator ($T = 3.5\,^{\circ}$C) and transferred to a container placed in a temperature-controlled water bath. A thermistor probe was inserted into one apple; the electrode pair was inserted into the other. In this way the spectra were not modified by the presence of the probe. Preliminary measurements indicated that the temperatures of the two apples agreed to within 0.1 °C. Spectra were taken for a large number of temperatures up to a maximum temperature, T_{max}. Spectra were also taken as the temperature was reduced to about 10 °C. Three different values were used for T_{max}: 34, 38 and 42 °C.

The diameter of an apple (approximately 8 cm) was considerably larger than the electrode needle length. The needles did not penetrate to the depth of the core. Little difference was thus observed in the impedance spectra of an apple with the electrodes oriented parallel to or perpendicular to the core. Furthermore, not all the needles penetrated completely into the apple because the rigid electrode configuration could not completely match the curvature of the apple surface. Because the electrode geometry did not change during the course of a temperature cycle, variations among apples in the penetration of the individual needles played no role in the determination of the enthalpies.

3. Impedance analysis

The interelectrode region can be regarded as a series combination of an electrode interface region and the bulk material region. To analyse the bulk properties, it is necessary to separate the contributions from these two regions. This separation is most readily accomplished by transforming the capacitance and conductance values to the equivalent impedance. The complex impedance, Z^*, can be written as the sum of a real part, Z_r, and an imaginary part, Z_i. $Z^* = Z_r + iZ_i$, where i is $-1^{1/2}$.

Considering a parallel equivalent capacitance and conductance, the impedance is related to the capacitance, conductance and frequency as follows

$$Z_r = G/(G^2 + \omega^2 C^2) \quad (1)$$

$$Z_i = -\omega C/(G^2 + \omega^2 C^2) \quad (2)$$

where $\omega = 2\pi f$.

Figs 2 and 3 illustrate the capacitance and conductance spectra of an apple at a temperature of 20.4 °C after it had been heated to 34 °C. Fig. 4 shows the corresponding impedance spectra. The spectra below and above about 100 Hz represent the contribution from the electrode and bulk regions, respectively. Fig. 5 indicates the circuit model used to represent the apple. Each region is modelled as the parallel combination of a resistance, R, and a constant-phase-angle element, CPE. Such a model has been used to describe the electrical behaviour of a wide variety of biological [5, 10] and non-biological systems [11, 12]. A resistance R_{hif} is added to account for the real part of relaxations which take place at frequencies above 1 MHz.

This circuit model represents the characteristics of the measured impedance spectra very well. The impedance of the CPE is given by $Z^*_{CPE} = A(i\omega)^{-n}$, where A and n are real-valued parameters. If X_{CPE} and Y_{CPE} represent, respectively, the real and imaginary parts of the CPE impedance, then $X_{CPE} = A\omega^{-n}\cos(n\pi/2)$ and $Y_{CPE} = A\omega^{-n}\sin(n\pi/2)$. The phase angle of the impedance, Φ, is given by $\tan\Phi = Y_{CPE}/X_{CPE} = \tan(n\pi/2)$. Thus, the phase angle of the CPE is

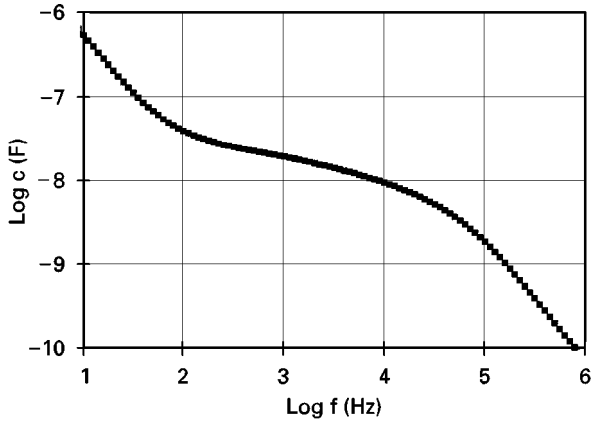

Figure 2 Capacitance spectrum for an apple heated to 34 °C, then cooled to 20.4 °C.

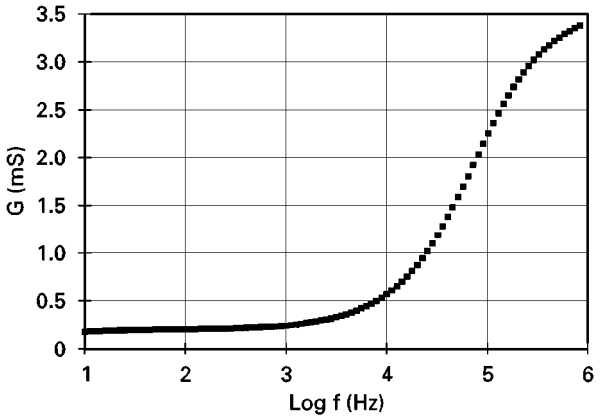

Figure 3 Conductance spectrum for an apple heated to 34 °C, then cooled to 20.4 °C.

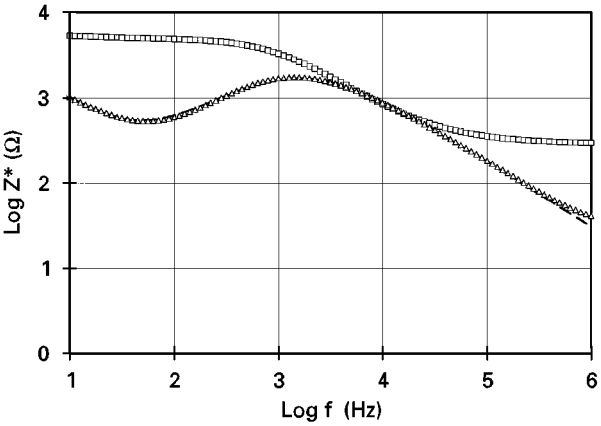

Figure 4 Impedance spectrum for an apple heated to 34 °C, then cooled to 20.4 °C. (□) ReZ measured, (△) ImZ measured, (——) ReZ calculated, (– – –) ImZ calculated.

a constant, $n\pi/2$, independent of the frequency. This result is the reason for the designation of this circuit element as a "constant phase element".

If $\mathrm{Re}Z_t$ and $\mathrm{Im}Z_t$ represent, respectively, the real and imaginary parts of the parallel CPE-resistance combination, then

$$\mathrm{Re}Z_t = R(X_{CPE}^2 + Y_{CPE}^2 + RX_{CPE})/D \quad (3)$$

and

$$\mathrm{Im}Z_t = Y_{CPE}R^2/D \quad (4)$$

where $D = (X_{CPE} + R)^2 + Y_{CPE}^2$.

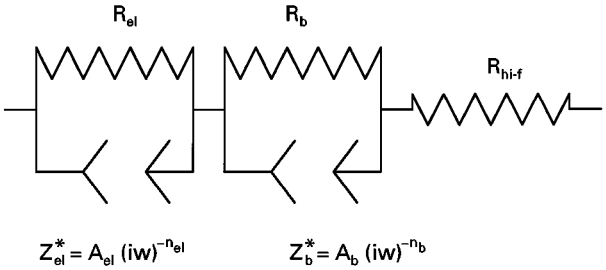

Figure 5 Circuit model used to calculate impedance spectra. "b" represents the bulk material between the electrodes, "el" represents the electrode/bulk interface. R_{hif} is an element used to represent relaxations which occur at frequencies above 1 MHz.

Equation 4 describes a peak in the imaginary part of the impedance at an angular frequency

$$\omega_p = (A/R)^{1/n} \quad (5)$$

with a full-width at half-maximum given by

$$\mathrm{FWHM} = R[\cos^2(n\pi/2) + 4\cos(n\pi/2) + 3]^{1/2}/\pi A \quad (6)$$

For frequencies $f \ll f_p$ the impedance of the CPE is relatively large and the parallel combination behaves as a pure resistance R. For $f \gg f_p$ the impedance of the CPE is relatively low. The combination then behaves as a pure CPE with both $\mathrm{Re}Z_t$ and $\mathrm{Im}Z_t$ decreasing as f^{-n}.

These asymptotic limits in the impedance spectrum can be related to the conductivity, g, as follows: for low frequencies $g \to g_{dc} \sim 1/R$; for high frequencies $g(\omega) \sim \omega^n/A$. Borsa *et al.* [13] have shown that the limiting behaviour of a system which exhibits a stretched exponential or Kohlraush–Williams–Watt (KWW) response, $\phi(t) \sim \exp[(-t/\tau)^{\beta}]$ in the time domain is $g_{dc} \sim \tau^{-1}$ at low frequencies and $g(\omega) \sim \omega^{(1-\beta)}\tau^{-\beta}$ at high frequencies. Equation 5 and the association $\tau = 1/f_p$ can then be used consistently to relate the parameters of the parallel CPE/R element and the KWW response according to $R \sim \tau^{-1}$, $n = 1 - \beta$, and $A \sim \tau^{\beta}$. The parallel CPE/R element thus serves as a circuit representation of the KWW response.

The region between 100 Hz and 100 kHz in Fig. 4 illustrates the frequency dependence given by Equations 3 and 4. A peak appears in the imaginary part of the impedance in the low kilohertz region. At lower frequencies, the real part of the impedance becomes constant and the imaginary part decreases towards zero. At higher frequencies the real and imaginary parts both exhibit a parallel, power-law decrease. The increase in the imaginary part below about 50 Hz indicates the beginning of a very low-frequency dispersion related to the electrode interface. The flattening of the real part above 100 kHz indicates the presence of a dispersion above 1 MHz, presumably related to coupling across the cell wall. The beginning of a corresponding rise in the imaginary part is apparent just below 1 MHz.

The seven circuit parameters shown in Fig. 5 (A_{e1}, n_{e1} and R_{e1} for the electrode region; A_b, n_b and R_b for the bulk midfrequency dispersion; and R_{hif} for the high-frequency impedance) provide a good fit to the

measured impedance over the frequency range from 10 Hz to 1 MHz. At each temperature, precise values for the seven parameters were obtained from a complex-valued, non-linear, least squares fit to the real and imaginary impedance values according to a method described by Bevington [14]. The results of such a fit are shown in Fig. 4 for comparison with the measured values. The agreement is very good. In fact, the solid line for the calculated values of ReZ cannot be seen beneath the measured values. In this manner, the temperature dependence of each parameter was obtained during the heating and cooling of each apple. The temperature variation of the peak frequency was then determined using Equation 5.

Fig. 6 illustrates impedance spectra for an apple heated to $T_{max} = 34\,^{\circ}C$ at three temperatures. As the temperature increases, ReZ at low frequencies and ReZ at high frequencies decrease. In addition, the peak in ImZ decreases in magnitude and shifts to higher frequencies.

The resistance values R_b and R_{hif}, can be converted to the corresponding conductivities, g_b and g_{hif}, from the relationship

$$g = Fd/SR \tag{7}$$

where F is a geometrical factor determined by the dimensions and arrangement of the needles in the array [8]. In this case $F = 23.3$. The electrode separation is d, and the geometrical area of each electrode is S.

Jain and Mundy [15] have shown that for glassy ionic conductors $g = B\exp(-H/kT)/T$ and $\omega_m = D\exp(-H_m/kT)$, where k is Boltzmann's constant, ω_m is the ion jump frequency, H_m is the enthalpy for ionic migration, H_f is the enthalpy for dissociation of the ion from its binding site (detrapping), and $H = H_m + H_f$. B and D are temperature-independent factors which depend on the entropies for migration and dissociation, the jump distance, the jump attempt frequency, and various geometric and correlation factors. Although their model was developed specifically for ionic glasses, the general temperature and enthalpy dependence of the ionic conduction processes should also be applicable to biological materials. Jain and Mundy note [15], for example, that in a liquid electrolyte, $H_f = 0$.

It should be noted that ω_p, obtained from the impedance analysis, is not the ion jump frequency, ω_m. The two, however, should be directly proportional and have the same activation enthalpy. Plots of $\ln(g_b T)$ versus $1/T$ and $\ln(\omega_p)$ versus $1/T$ should then yield as their slopes $H_m + H_f$ and H_f, respectively. Taken together, the two plots can be used to determine H_f and H_m and thus identify the relative contributions of detrapping and hopping to the conduction process.

4. Results

Figs 7–9 are Arrhenius plots for the bulk conductivity, peak frequency, and high-frequency conductivity, respectively, for an apple with $T_{max} = 34\,^{\circ}C$. Least-square fit lines used to determine the slopes are also shown. Several features are evident in these graphs. First, the slopes for increasing temperature are greater than the slopes for decreasing temperature. Second, at a given temperature the conductivities and the peak frequency are higher for decreasing temperatures than for increasing temperatures. The conductivity still decreases as temperature decreases, but at a slower rate after the maximum temperature has been reached. Raising the temperature has evidently resulted in an increased conductivity. Previous, less-detailed measurements [6] have shown similar results for apples heated to 35 °C.

Figs 10–12 are Arrhenius plots for the bulk conductivity, peak frequency, and high-frequency conductivity, respectively, for an apple with $T_{max} = 42\,^{\circ}C$. Several differences are immediately apparent from Figs 7–9. First, the slopes for increasing temperature and decreasing temperature appear similar in magnitude. Second, at a given temperature the conductivities and the peak frequency are lower for decreasing temperatures than for increasing temperatures. Raising the temperature has evidently resulted in a decreased conductivity. Third, a clear decrease in slopes is apparent in the graphs for the bulk conductivity and peak frequency between $1000/T = 3.25$ and 3.2 (34.5–39 °C). Between 39 and 42 °C the slopes are

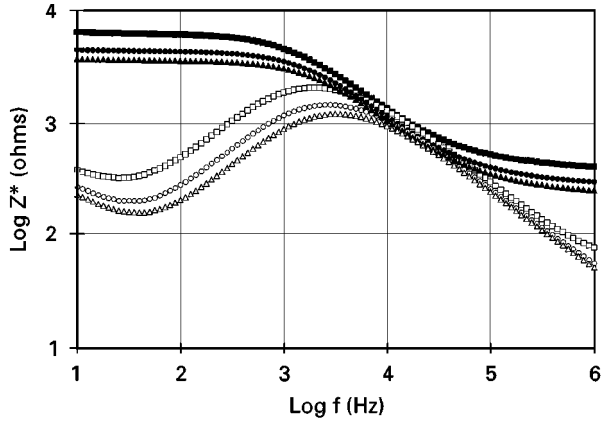

Figure 6 Impedance spectra for an apple being heated to 34 °C at three temperatures: (■) ReZ at $T = 9.5\,^{\circ}C$, (□) ImZ at $T = 9.5\,^{\circ}C$, (●) ReZ at $T = 22.4\,^{\circ}C$, (○) ImZ at $T = 22.4\,^{\circ}C$, (▲) ReZ at $T = 34.2\,^{\circ}C$, (△) ImZ at $T = 34.2\,^{\circ}C$.

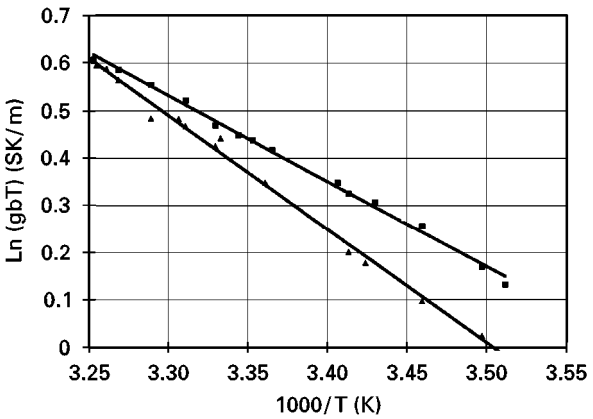

Figure 7 Arrhenius plots for the bulk conductivity of an apple heated to 34 °C: (▲) increasing temperature, (■) decreasing temperature.

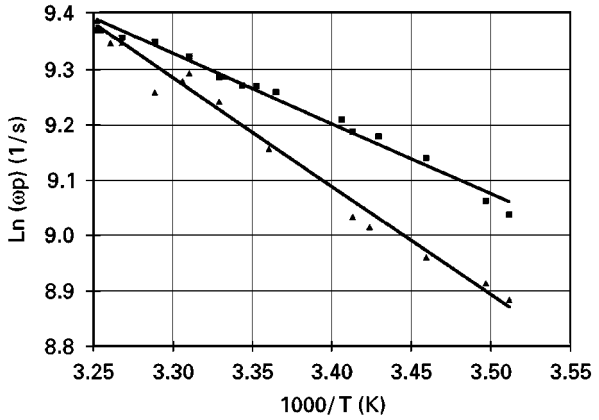

Figure 8 Arrhenius plots for the peak frequency of ImZ of an apple heated to 34 °C: (▲) increasing temperature, (■) decreasing temperature.

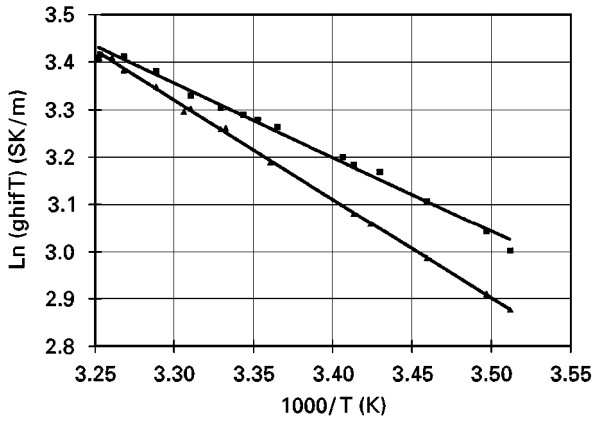

Figure 9 Arrhenius plots for the high-frequency conductivity of an apple heated to 34 °C: (▲) increasing temperature, (■) decreasing temperature.

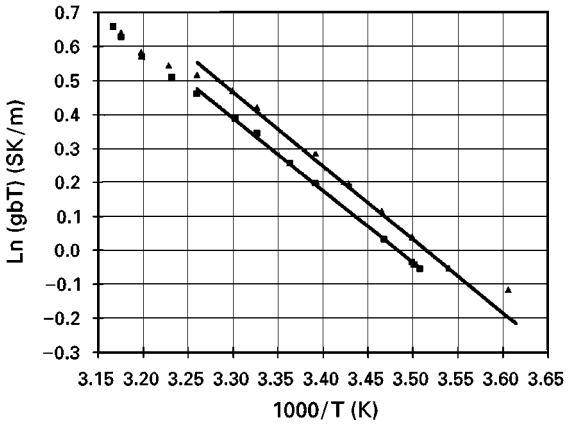

Figure 10 Arrhenius plots for the bulk conductivity of an apple heated to 42 °C: (▲) increasing temperature, (■) decreasing temperature.

similar to those below 34 °C. The slope of the high-frequency conductivity exhibits a smaller decrease between 34.5 and 39 °C. The difference between the curves for increasing and decreasing temperature is much more dramatic for the high-frequency conductivity.

For the apple with $T_{max} = 38$ °C, the behaviour is similar to that observed for the apple with $T_{max} = 42$ °C. The slopes for the corresponding graphs

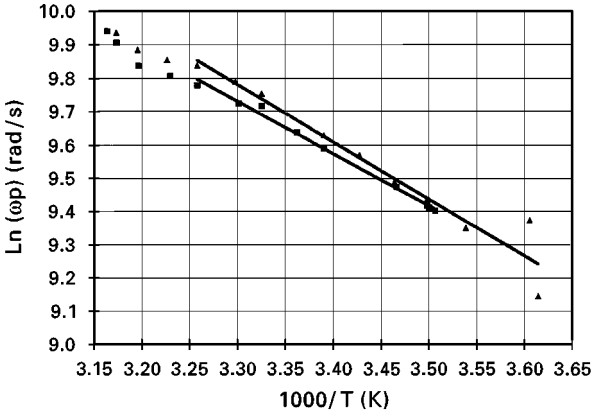

Figure 11 Arrhenius plots for the peak frequency of ImZ of an apple heated to 42 °C: (▲) increasing temperature, (■) decreasing temperature.

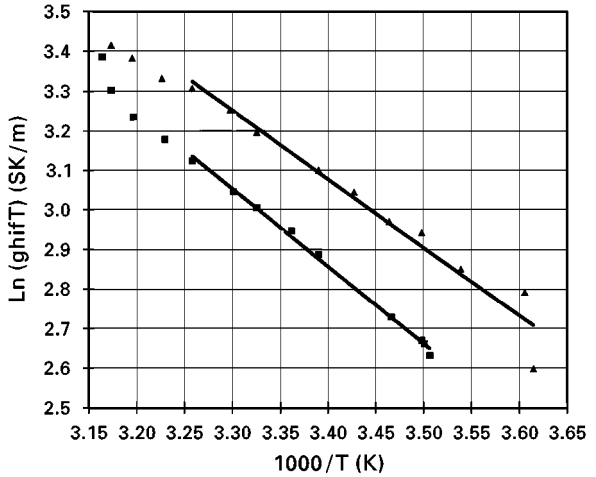

Figure 12 Arrhenius plots for the high-frequency conductivity of an apple heated to 42 °C: (▲) increasing temperature, (■) decreasing temperature.

(not shown here) are reduced between 34.5 and 38 °C. At a given temperature, the conductivities and the peak frequency are also lower for decreasing temperatures than for increasing temperatures. The differences, however, are greater than for the apple with $T_{max} = 42$ °C. For all three apples, n was independent of temperature and equal to 0.78 for both increasing and decreasing temperatures.

Table I presents the activation enthalpies for the bulk conductivity, the peak frequency for the bulk, and the high-frequency conductivity. The enthalpies associated with detrapping and hopping are determined from the analysis described above. Because the high-frequency peak appears at frequencies beyond the range of the present measurements, no value could be obtained for its ω_p. Thus, the activation enthalpy for the high-frequency process cannot be separated into detrapping and hopping enthalpies. For comparison, at room temperature, $kT \sim 0.025$ eV. The $\pm$ values indicated in Table I are the standard error values for the linear fit, which was performed using the Linest function of the spreadsheet program Excel. In all cases the slopes were determined only for temperatures below 35 °C.

TABLE I Activation enthalpies for apples heated to the indicated T_{max}

Parameters		Activation enthalpies	
	T_{max} °C	Increasing T	Decreasing T
g_b	42	0.185 ± 0.011	0.182 ± 0.002
ω_p		0.149 ± 0.013	0.136 ± 0.004
g_{hif}		0.149 ± 0.011	0.169 ± 0.004
H_m		0.149 ± 0.013	0.136 ± 0.004
H_f		0.036 ± 0.017	0.046 ± 0.004
g_b	38	0.178 ± 0.005	0.182 ± 0.002
ω_p		0.140 ± 0.006	0.124 ± 0.002
g_{hif}		0.159 ± 0.003	0.178 ± 0.002
H_m		0.140 ± 0.006	0.124 ± 0.002
H_f		0.038 ± 0.008	0.058 ± 0.003
g_b	34	0.207 ± 0.004	0.156 ± 0.003
ω_p		0.170 ± 0.007	0.110 ± 0.004
g_{hif}		0.182 ± 0.001	0.136 ± 0.004
H_m		0.170 ± 0.007	0.110 ± 0.004
H_f		0.037 ± 0.008	0.046 ± 0.005

5. Discussion

There are three major sources of error in the calculation of the activation enthalpy values for a particular apple: (1) errors in the determination of the slopes of the activation plots; (2) errors in the fitting procedure used to obtain the A, R and n values from the impedance data; and (3) errors in the measurement of the capacitance and conductance of the apples. The standard errors of the linear fits for the activation plots are indicated in Table I. The errors associated with the fitting procedure to determine the A, R and n values are calculated during the procedure [14]. The relative uncertainties are less than 1% for each of these values. Finally, the errors in the measurement of the capacitance and conductance by the impedance analyser are less than 1% over the frequency range of the bulk dispersion, as determined by measurements on standard resistor and capacitor combinations. Consequently, the error in the activation enthalpy values is due almost entirely to the determination of the slope of the activation plots, as given in Table I.

A series of runs was conducted to determine whether there was a significant drift with time in the impedance spectra. The fitted values of A_b, n_b, R_b and R_{hif} varied by less than 1% over a 2 h period for an apple at a temperature of 24.7 ± 0.2 °C. Preliminary measurements had shown, similarly, that the passive electrical properties of apples kept at room temperature did not vary appreciably until the onset of ripening (climacteric).

Another source of error is the individual variation of activation enthalpy values among different apples. This uncertainty can be estimated by comparing the activation enthalpies for increasing temperature for the three apples. Those values were obtained from fits for temperatures below 35 °C and should thus be similar. The H_f values for the three apples agree within the associated uncertainties. In contrast, the H_m value for the apple with $T_{max} = 34$ °C differs by about 20% from the other two apples. This amount exceeds the associated uncertainties and is probably a manifestation of a difference in the relative ripeness of the three apples. Consequently, any differences in H_m values less than 20% are of questionable significance. The activation enthalpies for bulk conductivity shown in Table I are also comparable in magnitude to the activation energies reported previously [6] for apples in the frequency range 100 Hz to 5 kHz.

In biological materials, the passive electrical properties in the kilohertz frequency range, represented here by g_b, ω_o, H_m and H_f, are determined by the hopping of ions along counterion layers at the surface of the cell wall or membrane [16]. At higher frequencies, represented here by R_{hif}, coupling across the cell wall or membrane becomes important.

For each apple in Table I, $H_m \gg H_f$. Furthermore, H_f is only slightly greater than kT (~ 0.025 eV). Consequently, changes in the conductivity with temperature are not the result of variations in the concentration of the ionic carriers, but are due to the temperature dependence of the ionic hopping mobility. The absence of a clear, significant difference in the H_f values for increasing and decreasing temperatures indicates that any structural changes produced by the heating do not affect the number of ionic carriers.

For each apple, H_m is lower for decreasing than for increasing temperatures. This decrease appears significant for the $T_{max} = 34$ °C apple, questionable for the 38 °C apple, but not significant for the 42 °C apple. Recall that the bulk conductivity was higher for decreasing than for increasing temperatures for the 34 °C apple and that the reverse was true for the other two apples. These differences and the changes in slope of the activation plots observed between 35 and 39 °C indicate that a structural change in the cell wall has occurred in that temperature range. This change is not reversible upon cooling and is thus not a simple phase transition. The total enthalpy for the high-frequency conductivity (g_{hif} in Table I) exhibits a similar difference in behaviour. It decreases significantly for the 34 °C apple, but increases significantly for the $T_{max} = 38$ and 42 °C apples.

Minor structural changes occur for apples heated up to 34 °C as is evident from the increased bulk conductivity during cooling observed here and previously [6] and by the lower values of H_m and the total enthalpy for high-frequency conductivity during cooling. Heating to temperatures in the range 35–39 °C, however, produces a more substantial change in cell-wall structure. During cooling, the bulk conductivity is reduced and the total enthalpy for high-frequency conductivity is increased, whereas H_m does not change. The temperature range in which these changes take place is similar to that observed for erythrocytes [5], but slightly lower than reported for rat muscle [4].

The values of the CPE exponent, n, and $\beta = 1 - n$ have been related to a variety of physical processes in models for ionic conduction in solids; for example, the distribution of transition rates [17], the degree of correlation of the ionic charge carriers [18, 19], and the ion–ion separation distance [20]. In the present case, n is independent of T and equal to 0.78, for each apple, both for increasing and decreasing temperatures. This result differs from the sharp variation of

n with T observed for erythrocytes [5]. This difference in results might indicate that the passive electrical properties of isolated cell culture systems are not the same as those properties measured in whole, living tissue. Alternatively, it may simply reflect a fundamental difference in the structure of cell membranes and walls.

Further research will investigate whether deterioration of the new cell-wall structure commences above 42 °C and whether there are additional structural changes in apples at higher temperatures. The association of shifts in electrical properties with structural changes in the cell wall/membrane should be studied for a wide variety of plant and animal systems. In particular, possible differences in the variation of the impedance spectra of warm-blooded and cold-blooded animals with temperature should be investigated. Finally, research should be directed toward examining the possible differences between the impedance spectra of cell cultures and intact tissue in living systems.

6. Conclusions

The results reported here indicate that the variation of the electrical properties of apples with temperature is determined by changes in the hopping mobility of the ionic carriers rather than a change in the number of the carriers. Furthermore, there is evidence of a structural change in the cell wall that occurs within the temperature range 35–40 °C.

7. Acknowledgements

This research was supported by a grant from the Howard Hughes Medical Institute Summer Research Science Programme. The assistance of Saurabh Dutta Chaudry with the analysis of the data is appreciated.

References

1. C.-M. LO, C. R. KESSE and I. GIAEVER, *Biophys. J.* **69** (1995) 2800.
2. Z.-G. QIAQ, L. MORKRID and L. K. VOLLESTAD, *Med. Bio. Eng. Comput.* **32** (1994) 161.
3. B. J. THOMAS, B. H. CORNISH and L. C. WARD, *J. Clin. Eng.* **17** (1992) 505.
4. D. A. MCRAE and M. A. ESRICK, *Int. J. Hyperthermia* **9** (1993) 247.
5. J.-Z. BAO, C. C. DAVIS and R. E. SCHMUCKLER, *Biophys. J.* **61** (1992) 1427.
6. F. X. HART and W. H. COLE, *J. Mater. Sci.* **28** (1993) 621.
7. F. X. HART and W. R. DUNFEE, *Phys. Med. Biol.* **38** (1993) 1099.
8. B. BODAKIAN and F. X. HART, *IEEE Trans. Diel. Elec. Ins.* **1** (1994) 181.
9. F. X. HART and B. BODAKIAN, *J. Mater. Sci. Lett.* **14** (1995) 1214.
10. F. X. HART, R. B. TOLL, N. J. BERNER and N. H. BENNETT, *Phys. Med. Biol.* **41** (1996) 2043.
11. J. B. BATES, D. LUBBEN, N. J. DUDNEY and F. X. HART, *J. Electrochem. Soc.* **142** (1995) L149.
12. B. WANG, J. B. BATES, F. X. HART, B. C. SALES, R. A. ZUHR and J. D. ROBERTSON, *ibid.* **143** (1996) 3203.
13. F. BORSA, D. R. TORGESON, S. W. MARTIN and H. K. PATEL, *Phys. Rev. B* **46** (1992) 795.
14. P. R. BEVINGTON, "Data Reduction and Error Analysis for the Physical Sciences" (McGraw-Hill, New York, 1969).
15. H. JAIN and J. N. MUNDY, *J. Non-Cryst. Solids* **91** (1987) 315.
16. K. R. FOSTER and H. P. SCHWAN, *CRC Crit. Rev. Biomed. Eng.* **17** (1989) 25.
17. J. R. MACDONALD, *Phys. Rev.* **B49** (1994) 9428.
18. K. FUNKE, *Prog. Solid State Chem.* **22** (1993) 111.
19. K. L. NGAI and R. W. RENDELL, *J. Molec. Liq.* **56** (1993) 199.
20. H. K. PATEL and S. W. MARTIN, *Solid State Ionics* **53–56** (1992) 1148.

Received 28 May 1997
and accepted 15 May 1998